

1 **Novel feature selection methods for construction of accurate**
2 **epigenetic clocks**

3

4 **Adam Li, Alice E Kane, Amber Mueller, Brad English, Anthony Arena, Daniel Vera, David A**
5 **Sinclair**

6

7 **Affiliations**

8 Blavatnik Institute, Dept. of Genetics, Paul F. Glenn Center for Biology of Aging Research at
9 Harvard Medical School, Boston, MA

10

11 **Abstract:**

12 Epigenetic clocks allow the accurate prediction of age based on the methylation status of specific
13 CpG sites in a variety of tissues. These predictive models can be used to distinguish the biological age of
14 an organism from its chronological age, and are a powerful tool to measure the effectiveness of aging
15 interventions. There is a growing need for methods to efficiently construct epigenetic clocks. The most
16 common approach is to create clocks using elastic net regression modelling of all measured CpG sites,
17 without first identifying specific features or CpGs of interest. The addition of feature selection
18 approaches provides the opportunity to reduce the cost and time of clock development by decreasing the
19 number of CpG sites included in clocks. Here, we apply both classic feature selection methods and novel
20 combinatorial methods to the development of epigenetic clocks. We perform feature selection on the
21 human whole blood methylation dataset of ~470,000 CpG features published by Hannum and colleagues
22 (2015). We develop clocks to predict age, using a variety of feature selection approaches, and all clocks
23 have R² correlation scores of greater than 0.73. The most predictive clock uses 35 CpG sites for a R²
24 correlation score of 0.87. The five most frequent sites across all clocks are also modelled to build a clock
25 with a R² correlation score of 0.83. These two clocks are validated on two external datasets where they

26 maintain excellent predictive accuracy and outperform Hannum et al's model in accuracy of age
27 prediction despite using significantly less CpGs. We also identify the associated gene regulatory regions
28 of these CpG sites, which may be possible targets for future aging studies. These novel feature selection
29 algorithms will lower the number of sites needed to be sequenced to build clocks and allow
30 conventionally expensive aging epigenetic studies to cost a fraction of what it would normally.

31

32 **Introduction:**

33 Epigenetic clocks allow for the prediction and observation of biological aging (Bocklandt, 2011).
34 By profiling the methylation levels at specific sites in DNA, it is possible to accurately predict the age of
35 organisms and tissues (Horvath 2013). This is often referred to as epigenetic or DNA methylation
36 (DNAm) age. CpG sites are areas of repetitive DNA bases where a guanine follows a cytosine, which
37 can be modified via DNA methylation and demethylation to alter the structure of chromatin and gene
38 expression in a cell (Moore et al., 2021). Epigenetic clocks can now predict age across multiple species
39 and tissue types (Thompson et al., 2018), and even predict mortality (Lu, Quach et al 2019). With the
40 increased use of DNA methylation clocks to determine biological age and screen for interventions that
41 slow or reverse aging the demand for more robust, accurate clocks is growing.

42

43 The first epigenetic clocks were created by Bocklandt et al (Bocklandt et al, 2011) and quickly
44 followed by the Hannum and Horvath labs in 2013 (Hannum et al, 2013; Horvath 2013). The Hannum
45 clock, based on methylation analysis of DNA from peripheral blood mononuclear cells, was developed
46 using elastic net regression modelling. 71 markers were selected from over 470,000 CpG sites to derive
47 an age prediction accuracy of four years (Hanuum et al. 2013). Horvath's clock encompasses multiple
48 tissue types and includes 353 CpG sites that strongly predict age (Horvath 2013). Recently, there has
49 been a focus on creating clocks with fewer CpG sites to enable epigenetic age profiling without the use of
50 costly microarrays or expensive reduced-representation bisulfite sequencing (Ito el al. 2018, Park JL, et al.
51 2016, Zbieć-Piekarska et al. 2014, Spólnicka, M. et al. 2017). Alghanim et al.'s clock, built on blood

52 methylation data, only uses CpG sites from three gene regions to explain 84-85% of age variance
53 (Alghanim et al. 2017), and Weidner's clock based on only 3 CpG sites, is able to predict age with an
54 error of less than five years (Weidner et al., 2014).

55

56 Few epigenetic clock studies employ a discrete step to find optimal features for building clocks.
57 Feature selection is commonly used in situations where the number of features far outnumber the number
58 of samples (Guyon et al. 2003). Given the vast number of CpG sites in the genome and the relatively low
59 number of samples in most studies, feature selection methods will improve the efficiency of clock
60 building. Currently, the most common approach for clock building is to use a 'correlation-with-age'
61 method, where CpGs that have a non-zero coefficient in ElasticNet Regression analyses are given more
62 predictive power in the model (Horvath 2013, Hannum et al. 2013). Some clocks utilize more advanced
63 feature selection methods such as Boruta (Renner et al., 2013), recursive feature selection (Wang et al.,
64 2018; Darst, Malecki and Engelman, 2018; Meng, Murrelle and Li, 2008) or neural networks (Spólnicka
65 et al. 2017). These algorithms select even fewer CpG features whilst still accurately predicting age.
66 However the number of clocks being built with these tools is minimal and there is more room to optimise
67 feature selection methods and parameters.

68

69 Here, we use several feature selection approaches to construct accurate epigenetic clocks with
70 low numbers of CpG sites on the publicly available Hannum dataset (GSE40279), and evaluate their
71 accuracy and generalizability on other datasets: GSE52588 (Horvath et al, 2015), GSE137688 (McEwen
72 2019), GSE85311 (Martens et al, 2020). We use a combination of modified standard methods that are
73 readily available in python packages as well as the development of our own novel selection methods. We
74 combine methods and use them in tandem to form new methods of feature selection, and optimise the
75 development of epigenetic clocks to predict age.

76

77 **Results:**

78 In order to test how few CpG sites could be selected while retaining predictive accuracy, we
79 applied each of our feature selection methods to the Hannum methylation dataset (GSE40279). Table 1
80 and Figure 1 summarise the results of the feature selection approaches, including the number of CpG
81 sites identified with each approach, and the correlation (r^2) with chronological age on a test set. The best
82 model for age prediction for this dataset is *SelectKBest for 2000 features followed by Boruta*. This
83 approach selects 35 CpG sites, with an r^2 of 0.873 and a median absolute error of 3.08 years (Table 1).

84

	Average R2 Score (from 10CV)	STD (Years)	Mean Absolute Error (Years)	Median Absolute Error (Years)
KBest 2000 de novo then Boruta (35)	0.873	0.05	3.82	3.08
Intersection of all methods per CV fold then Boruta (102)	0.865	0.06	3.9	3
KBest 25 de novo (36)	0.862	0.06	3.96	3.14
Boruta de novo (53)	0.861	0.06	3.95	3.08
%-RFE de novo to 1500 then Boruta (52)	0.835	0.07	4.35	3.57
ElasticNet de novo/No Feature Selection (276)	0.827	0.06	4.64	3.91
%-RFE de novo to 100 (161)	0.825	0.07	4.69	3.83
Top 10 Most Frequent (10)	0.825	0.08	4.59	3.7
Top 5 Most Frequent (5)	0.82	0.08	4.6	3.79
%-RFE de novo to 10000 then Genetic Algorithm (54)	0.818	0.08	4.61	3.76
SFM ElasticNet de novo then Boruta (7)	0.813	0.07	4.7	3.71

Genetic Algorithm de novo (85)	0.812	0.08	4.72	3.68
SFM ElasticNet de novo (16)	0.81	0.07	4.74	3.84
%-RFE de novo to 1500 then SFM (16)	0.81	0.07	4.74	3.84
SFM ExtraTrees de novo (5)	0.77	0.08	5.36	4.27
SFM ExtraTrees de novo then Boruta (5)	0.77	0.08	5.36	4.271
Neural Network feature selection (65)	0.76	0.08	5.65	4.79
Post Feature Selection Intersection of all methods (1)	0.73	0.09	5.75	4.38
Variance Threshold de novo (2)	0.02	0.02	11.9	10.61

85 **Table 1.** Results from feature selection methodology (in descending order of correlation scores).

86

87 Our other feature selection methods, including most of the SelectFromModel (SFM) methods, the
88 genetic algorithms and several combinations of methods, achieve an accuracy of between 0.77 to 0.82
89 (Table 1). Despite being fundamentally different in their approach, these methods accomplish similar
90 results and plateau in the same range of scores (Figure 1). Further optimization of each of these methods
91 is needed to warrant their usage over other more successful methods.

92

93 *ElasticNet de novo* (Table 1, Figure 1) represents a model without any feature selection methods
94 for comparison to the other models. This model uses all ~450,000 features to train a model without any
95 pre-selection or iterative algorithms. The resulting clock from this approach is based on 276 CpGs, which
96 is a much higher number of CpGs than clocks developed with the feature selection methods (Table 1),
97 and with a lower r2 score than five of the feature selection models (Table 1).

98

99 The majority of Recursive Feature Elimination (RFE) and Boruta based methods score 0.82 or
100 higher suggesting that for this dataset these methods work best (Table 1). Boruta de novo and KBest 25

101 de novo score remarkably well with no prior method being applied (0.861 and 0.862 respectively). These
102 are the best performing solo feature selection methods.

103

104 Using the five most frequently-selected CpGs among all the methods to build a clock gave a
105 correlation score of 0.83 and median absolute error of 3.79 years (Table 1). Table 2 shows the
106 corresponding GeneIDs for these CpGs. The most frequent CpG site is cg16867657 (ELOVL2) and
107 training a clock on this single feature results in a correlation score of 0.73 (Table 1). Overall, these results
108 demonstrate that using feature selection methods accurate epigenetic clocks can be constructed with only
109 a few CpGs.

110

Most Frequent 5 CpG Sites	Associated GeneID
cg16867657	ELOVL2
cg10501210	C1orf132
cg22454769	FHL2
cg04875128	OTUD7A
cg19283806	CCDC102B

111 **Table 2.** Table showing the 5 CpG sites that are chosen as most frequent predictors for aging and their
112 associated gene symbols

113

114 We also tested a neural network approach for feature selection. An ElasticNet Regression model
115 trained on the top 65 features selected by the neural network, has a moderate r² value of 0.76.
116 Interestingly, only four of the 65 identified neural network CpGs overlap with the CpGs selected by other
117 methods described here. Given a neural network's unique ability to detect these CpG sites as predictors,
118 this is a promising predictive tool to uncover more obscure CpGs that most conventional methods miss.

119

120 We selected two models developed above for further validation of their accuracy in independent
121 datasets. *SelectKBest for 2000 features followed by Boruta & the top 5 most frequent features* are the best
122 performing feature selection method and the clock with the lowest number of CpGs sets, respectively.
123 We applied these two clock models to two published blood methylation datasets. GSE85311 is
124 methylation profiling of blood taken from young and old human subjects of varying exercise level
125 (Martens et al, 2020). GSE52588 is methylation profiling of blood taken from subjects with and without
126 down syndrome (Horvath et al, 2015). Each of the clocks predicted age very well in these external data
127 sets with R2 values greater than 0.93 (Table 3, Figure 2), performing better than Hannum's final
128 published clock created from 71 CpG sites (Hannum 2013), despite using far fewer features.

129

Feature Selection Methods	Data set	r2 Score	Mean Absolute Error (Years)	Median Absolute Error (Years)
KBest 2000 de novo then Boruta (35)	GSE85311	0.931	4.66	4.18
	GSE52588	0.946	3.35	2.68
	GSE137688	0.710	2.0	1.6
Top 5 Most Frequent (5)	GSE85311	0.964	5.71	5.60
	GSE52588	0.932	4.56	3.98
	GSE137688	0.470	2.72	2.29

130 **Table 3.** Table showing the results of the two final models trained on the Hannum dataset (GSE40279,
131 Hannum et al 2013) validated on external datasets: Horvath down syndrome blood dataset (GSE52588,

132 *Horvath et al, 2015), Martens exercise blood dataset (GSE85311, Martens et al, 2020), and buccal*
133 *dataset (GSE137688, McEwen 2019). Number of CpG sites/features in parentheses.*

134

135 To test whether clocks developed with our feature selection approaches can be applied to datasets
136 other than those developed in blood, the two selected models above were also applied to a buccal cell
137 dataset (GSE137688, (McEwen 2019)). Using the methods on this dataset, we achieved a top r2 score of
138 0.71 with the *SelectKBest for 2000 features followed by Boruta* method and r2 of 0.47 with the *Top 5*
139 *Most Frequent* method (Table 3). The scores were expectedly lower than the results of the other two
140 validation sets because the clocks were trained on blood data, and applied to buccal swab data, which
141 have inherent sampling and variance differences. While the r2 scores were not as high, the models did
142 have very low mean and median absolute errors; the lowest of all results in this paper. Given the
143 abundance and ease of access buccal samples provide, this is promising rudimentary groundwork for the
144 application of feature selection methods on sample types beyond blood.

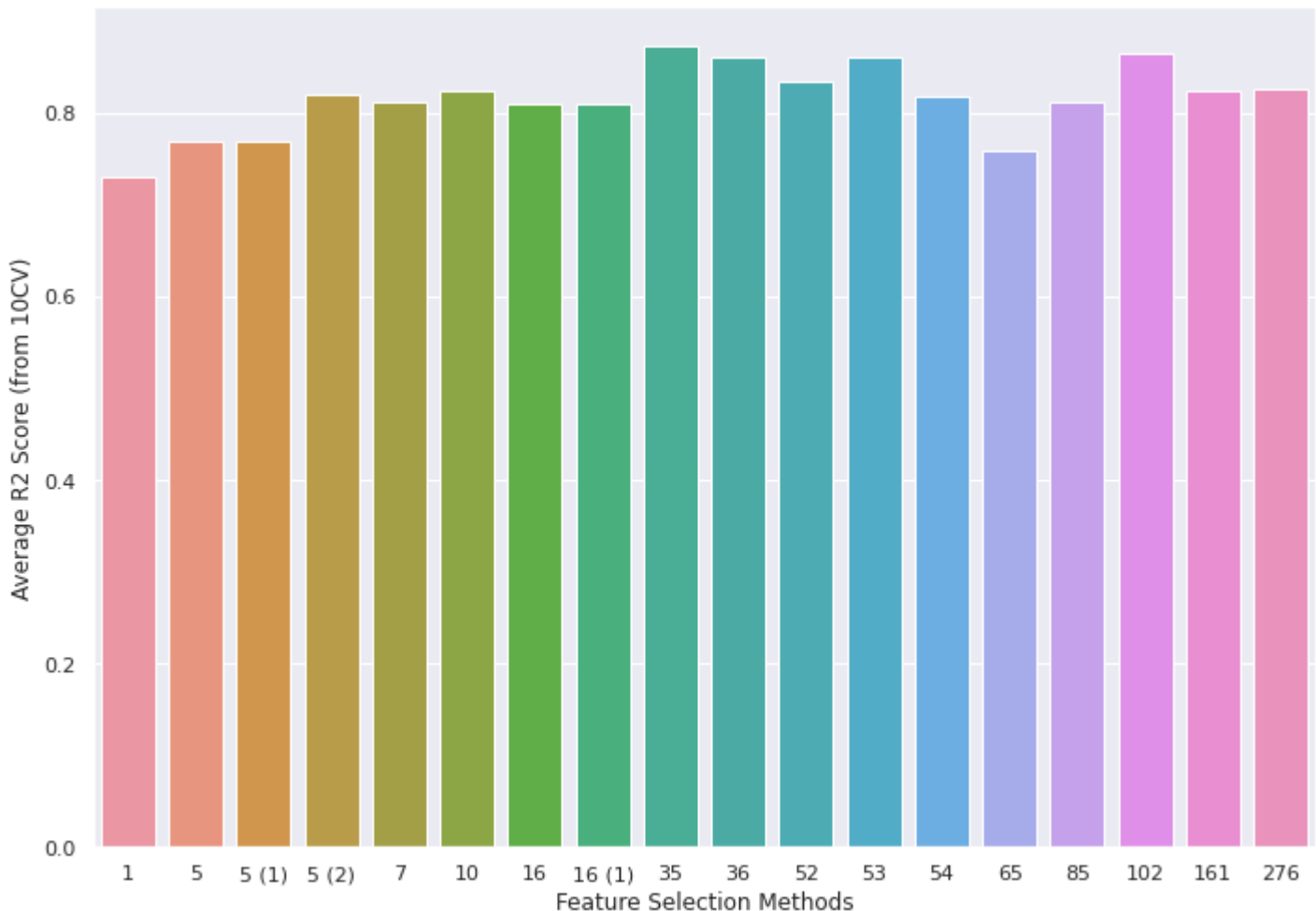
145

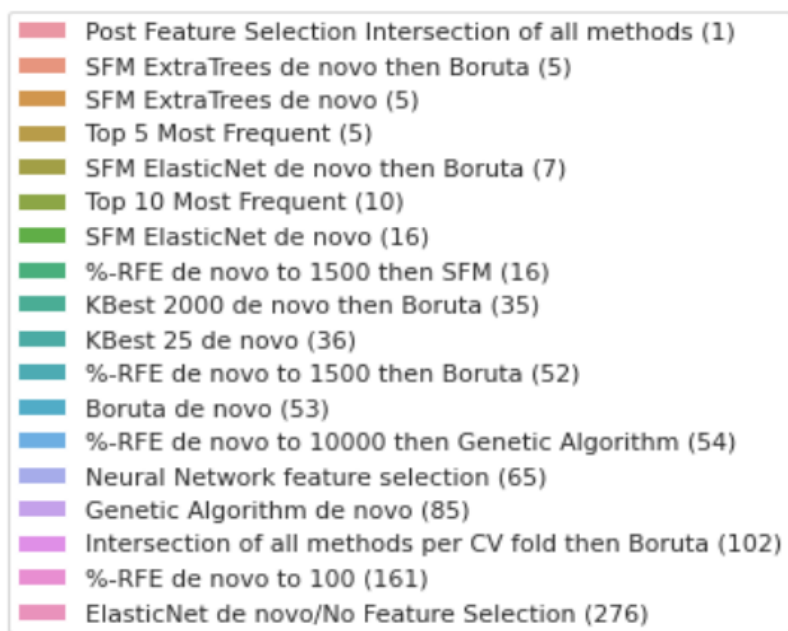
146 We next wanted to test whether the features selected with our methods, could be used to make
147 accurate clocks in other datasets. We took the CpGs selected from the Hannum dataset using our top two
148 models (SelectKBest for 2000 followed by Boruta & the top 5 most frequent CpG features), and selected
149 those same CpGs in the Horvath down syndrome dataset (GSE52588, Horvath et al, 2015). Using only
150 those CpGs, we created a clock from that remaining dataset, using the same cross-validation scheme (see
151 Methods) used for the original Hannum experiment above. Remarkably, clocks developed in this dataset
152 based on 35 features (SelectKBest for 2000 features followed by Boruta) and 5 features (top 5 most
153 frequent) achieved r2 scores of 0.928 and 0.911 respectively (Table 4). This shows these CpGs can be
154 used across datasets to create accurate clocks and are possibly universal, non-dataset specific CpGs for
155 predicting age.

156

Feature Selection	Average R2 Score (from 10CV)	Mean Absolute Error (Years)	Median Absolute Error (Years)
Method CpGs used			
KBest 2000 de novo then Boruta (35)	0.928	3.39	2.92
Top 5 Most Frequent (5)	0.911	4.02	3.72

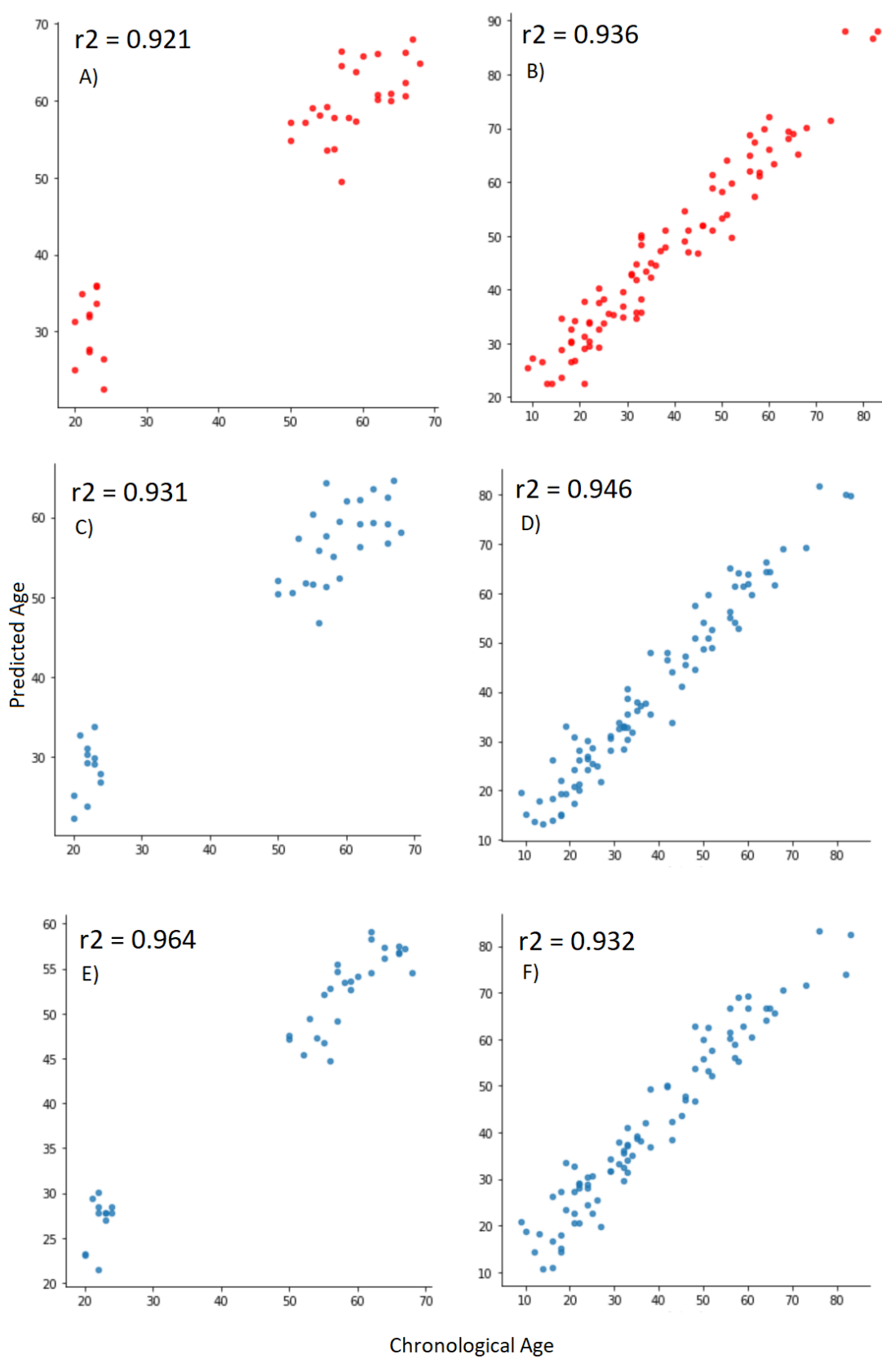
157 **Table 4.** Table showing the results of the two models created from the Horvath down syndrome blood
 158 dataset (GSE52588, Horvath *et al*, 2015) using the same CpGs selected from the two feature selection
 159 methods from the initial Hannum experiment. These models were validated using the same 10CV scheme
 160 from the initial Hannum experiment. Number of CpG sites/features in parentheses.





162

163 **Figure 1.** Figure showing the comparative methods with the number of features used in each model on
164 the x-axis and their average R2 scores on the y-axis. R2 scores are relatively similar across the board
165 despite the number of features needed for prediction varying widely.



167 **Figure 2.** *Figure showing the Predicted Ages vs Chronological Ages results of the two final models and*
168 *Hannum's model on the two external validation datasets GSE85311 and GSE52588. (A-B) Hannum (C-*
169 *D) KBest 2000 de novo then Boruta (E-F) Top 5 Most Frequent.*

170 **Discussion:**

171 Overall we show feature selection methods can select CpG sites that are highly predictive of age,
172 allowing for less features needed to build an accurate epigenetic clock. Many different types of feature
173 selection methods are able to attain a reasonably high correlation score of around 0.75-0.85 whilst using a
174 low number of CpG features. The rudimentary base code that outlines most of the feature selection ideas
175 in this paper is publicly available and we hope that feature selection becomes a standard discrete step in
176 future epigenetic clock studies. The corresponding genes of the most common CpG sites in these clocks
177 are possible future targets for aging studies.

178

179 Two of our clocks, both trained on the original Hannum dataset, also performed well on two
180 external datasets. The models, in fact, performed higher on validation datasets than the training dataset,
181 and outperformed Hannum's original clock that uses 71 features. This validates both the feature selection
182 methods' ability to reliably select good CpGs and the construction of our clocks. These clocks are thus
183 able to be used by others reliably to serve as predictors of chronological age. We also applied these
184 models to a dataset of a different sample type; buccal epithelial cells. Although the r² scores were only
185 moderate for this dataset, the mean and median absolute errors were the lowest we observed. This
186 suggests an interesting future potential for buccal/saliva methylation samples, as they are much more
187 accessible and less expensive to obtain.

188

189 In addition to the validation of the clocks, we also tested whether the identified CpGs of two of
190 these methods could be used to make accurate clocks using the Horvath down syndrome dataset (Horvath
191 et al, 2015, GSE52588). These clocks still achieved high 0.91-0.92 r² scores (Table 4). This suggests that

192 these features and their ability to predict age are not dataset specific and can universally be used across
193 other methylation datasets.

194

195 We identified five CpGs and their corresponding genes that were of particular interest, as they
196 were most commonly identified across all feature selection methods in our study (Table 3). Four of these
197 CpG sites, and particularly ELOVL2, have been previously identified as strong predictors of age.
198 ELOVL2, C1orf132, FHL2 and CCDC102B are included in an online seven CpG site epigenetic clock
199 from the University of Santiago de Compostela (Mathgene, 2021). Zbieć-Piekarska et al constructed a
200 linear regression model using only ELOVL2's CpG site (cg16867657) to predict age (Zbieć-Piekarska et
201 al., 2015) and obtained a high degree of accuracy in blood samples from humans. By manipulating the
202 expression of ELOVL2 and observing age-related changes in the eyes of mice, Chen et al suggest that the
203 gene is a molecular regulator of aging in the retina. Spólnicka and colleagues used ELOVL2 to accurately
204 detect age differences from 3 disease groups (Spólnicka et al., 2018), and also highlight C1orf132 and
205 FHL2 as key genes from which CpG sites are used for their epigenetic clock. CCDC102B also has links
206 to aging and age-related degenerative diseases (Hosoda et al., 2018, Xia et al., 2018). Ito and colleagues
207 developed a clock using only the CpG sites associated with CCDC102B and ELOVL2 (Ito et al., 2018)
208 and are able to predict age with an r^2 of 0.75. Additionally, Fleckhaus et al.'s study develops a clock
209 using 8 target regions, four of which are ELOVL2, FHL2, CCDC102B and C1orf132 (Fleckhaus et al.,
210 2020). These papers show that our feature selection methods are able to select the most age-predictive
211 CpG sites, consistently with other studies.

212

213 OTUD7A is the fifth gene of interest that we identified with our methods, but is the least
214 documented. One study has previously identified that high methylation rates of CpG sites associated with
215 OTUD7A are correlated with age (Tharakan et al., 2020), and Yin et al. identified it as a potential
216 regulator for neurodevelopmental disorders (Yin et al., 2018). The role of OTUD7A in aging, if any, is
217 not well-known and should be explored further.

218

219 We also applied a neural network method for feature selection in this study, but found it was not
220 as powerful in terms of predictive accuracy as the other feature selection methods. However, this method
221 did select many CpG features that were missed by our other conventional and novel methods. As neural
222 network architecture becomes more advanced in its ability to read in larger datasets, the features it selects
223 may eventually rival the accuracy of other methods. The features identified with neural networks may
224 also give rise to new sets of CpG sites and genes worthy of study in aging.

225

226 The feature selection methods we introduce here overcome the common computational issues of
227 stock selection methods and select a low-number of CpG sites whilst still yielding predictions of age that
228 have high accuracy. These methods can be applied to a range of future studies developing epigenetic
229 clocks including across new tissue types, or by examining a limited subset of CpGs in mutual overlap
230 between bulk methylation and single cell datasets (Trapp et al, 2021). Parallelized, highly cost-reduced
231 methods targeting specific CpG regions (Griffin et al. 2021) are another prime example. Lastly, these
232 methods are not limited to the identification of CpG sites as features, and this pipeline could be used to
233 identify features for biomarkers or clocks developed from a range of datasets (eg. metabolomics,
234 microbiome, clinical data), and to predict a variety of age and health outcomes.

235

236 **Methods:**

237 Data

238 The datasets for this study are from the Gene Expression Omnibus database under the accession
239 codes GSE40279, GSE85311, GSE52588 and GSE137688. The main dataset GSE40279 we test the
240 feature selection methods on contains 656 samples (instances) of whole blood human methylation levels
241 at 473,035 CpG Sites (features), matched to chronological ages. All analysis was done in Python 3. All
242 related code outlining our methods is available on github (<https://github.com/adamyli/CLK-MKR>).

243

244 Cross-validation and overall approach

245 The main workflow methodology is outlined in Figure 3. The original dataset was split into 10
246 folds for cross-validation (CV). For each set of training folds, every different feature selection method
247 was performed to select the optimal features within that training data. For every CV iteration, the
248 intersection of each feature selection method was also recorded and we performed Boruta on the
249 intersected features. For each of the feature selection methods, the resulting unique features from each
250 of the 10 iterations were collected into an aggregated list and entered into a final results dataframe. This
251 dataframe contains every unique feature selected by each selection method at each of the 10 iterations.

252

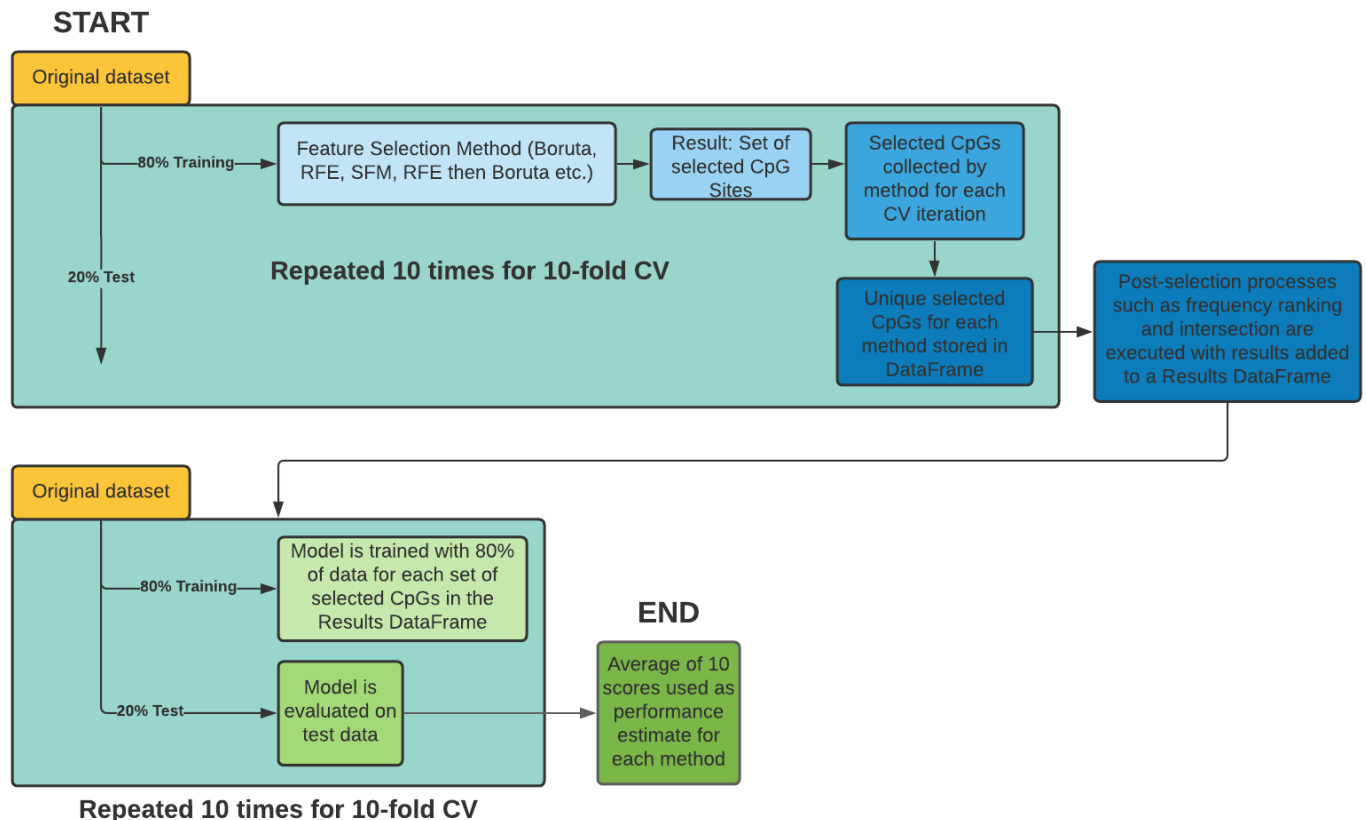
253 Post-feature selection processes were then performed. These include the intersection between the
254 results of all selection methods and ranking the top 5 and 10 most common features out of all the results.
255 The results from these two post-feature selection processes were also added to the Results Dataframe.
256 The original dataset was split into 10 folds again and for each column of the Results DataFrame, which
257 represents the unique selected features for every method, we reduced the dataset down to the selected
258 features. We trained the ElasticNet regression model for chronological age using training data (80%) and
259 evaluated the model on the test data (20%) using the r2 scoring metric. For each column the mean of the
260 10 r2 scores was the performance estimate of that feature selection method.

261

262 The best performing model was the clock from the *SelectKBest method down to 2000 features*
263 *followed by Boruta* resulting in 35 selected features. The second model of interest uses the top 5 most
264 frequently selected CpGs. These 2 models were validated using two external blood methylation datasets;
265 (GSE52588) and (GSE85311) and their performance was compared to Hannum's model's predictions on
266 these two datasets. The features from these two models were also used to build models from the
267 GSE52588 dataset and predict age using the same 10-fold CV as the Hannum dataset to investigate if
268 these selected features are effective across datasets.

269

270 These two models are also applied to a methylation dataset taken from buccal cells (GSE137688)
271 to see if performance could be replicated in conventionally cheaper samples (McEwen 2019).
272



273
274 **Figure 3.** The workflow for feature selection and model evaluation. Feature selection was performed on
275 training data for each iteration of 10-fold cross validation. The selected features of each iteration are
276 aggregated into a list for each feature selection method type. The unique selected features for each
277 method are collected into a dataframe where post-selection processes such as intersections are
278 performed. We add the results to a dataframe. Each column of selected features in the results dataframe
279 (each representing a different feature selection method) is tested using another training-testing split on
280 the original data. This is done 10 times for 10-CV with the average of all scores being the performance
281 estimate for that feature selection method.

282

283 Feature selection methods:

284 SelectFromModel (SFM):

285 SFM is a function within skLearn (Pedregos et al., 2011) that wraps around and trains a model on
286 a dataset and allows the user to specify a threshold of feature importance. Depending on whether the
287 model is a standard regression or random forest model, the feature importance is calculated from the
288 coefficients or mean importance respectively. Features (CpG sites) with less feature importance than this
289 threshold are discarded, leaving only the features with the highest coefficient or importance. This method
290 is fast but simple. Thresholds of 0.01, 0.05, 0.1, 0.5 are tested. For this study, the models that the SFM
291 wraps around are ElasticNet Regression and ExtraTrees forest.

292 The ExtraTrees Regression estimator is composed of a number of decision trees. A decision tree
293 can be thought of as an intuitive flowchart where an answer to one decision between 2 or more choices
294 leads to another. Decision trees decide how to split by prioritizing the split that creates the least uniform
295 distribution of labels or values. This branching of nodes continues until it reaches a node that cannot
296 decide which split to use because they result in equally uniform distributions - meaning any more
297 branches will not help the tree make any better decisions. In this sense ExtraTrees is similar to the more
298 popular random forest with a few distinct differences. Random Forest samples the training data with
299 replacement to train their decision trees while ExtraTrees uses the entire original dataset. However
300 ExtraTrees randomly chooses the split instead of optimally finding a locally one which is what Random
301 Forest does. ExtraTrees are therefore less exhaustive in their optimization and are faster than Random
302 Forests. This is ideal for us as a Random Forest with 5-8 trees in it can take several hours to train on a
303 dataset as large as ours. A random forest takes an advantage known as bagging by taking random
304 instances of the dataset and training its model from solely those samples. For a regression problem like
305 ours the average value of all trees are taken as the final prediction.

306
307 Recursive Feature Elimination (RFE) and the introduction of %-RFE:

308 RFE is a function that trains a model on a dataset and removes the weakest feature based on the
309 lowest feature importance from the dataset (Pedregos et al., 2011). This new dataset of N-1 features is

310 trained again with a model and the process is repeated until only the user specified number of features is
311 left. By removing 1 feature each time, RFE is a brute force algorithm that leaves only the best performing
312 features at each iteration. However it does not take into account all features at the same time, and is
313 unable to be aware of relationships between CpGs when it comes to predicting age e.g. some CpGs may
314 become a strong predictor of ageing in the presence or absence of another.

315 Applying the stock RFE algorithm to our dataset of 473,035 features is computationally limiting
316 due to the size of the dataset (Supplementary Table 1). Instead, we write an algorithm that removes a
317 percentage-based number of features at each iteration allowing us to aggressively remove the majority of
318 unnecessary features at the start but be more meticulous with our selection near the end. The percentage
319 chosen is 1%, i.e. removing 4730 features at 473,035 and 1 feature at 100.

320

321 Boruta:

322 RFE is a ‘minimal optimal’ feature selection method, meaning it attempts to select the smallest
323 set of features with the minimum error for an estimator and aims to optimize this ratio. Boruta differs as
324 an ‘all-relevant’ feature selection method compatible with only tree-based regression methods, such as
325 random forests (Kursa et al., 2010). Instead of trying to find the most compact set of features to predict
326 with, it considers all features that could possibly contribute towards prediction overcoming the weakness
327 of RFE’s greedy nature. Boruta creates duplicates of the existing features with randomized values called
328 ‘shadow features’. The dataset comprising the original and the shadows, is trained on the tree estimator
329 and the shadow features compete with their original forms. Features that consistently beat their shadow
330 counterparts are selected as reputable predictors. In order to deal with the computational power needed to
331 train a random forest with over 470,000 features, we use fewer trees and adjusted iteration counts in these
332 models.

333

334 SelectKBest:

335 SelectKBest is a feature selection method in sklearn similar to SFM that fits a dataset and selects
336 features based on a scoring metric (Pedregos et al., 2011). For each feature it calculates the correlation
337 value between the feature and target label and ranks them. This method is fast due to its shallow nature
338 of only training once so is not useful when used alone. However, it is helpful to reduce the total number
339 of features for usage of more greedy algorithms such as Boruta. In our methodology we select the top 25
340 features and the top 2000 features using SelectKBest. We perform Boruta on the top 2000 features.

341

342 Variance Threshold:

343 Variance threshold is a simple and exploratory method that removes all features whose column
344 of values do not reach the threshold of variance (Pedregos et al., 2011). Since some datasets naturally
345 may not have a high degree of variance in their recorded data, this method is not consistent. However
346 since its execution is the fastest out of all the methods (Supplementary Table 1) it is included as an added
347 method.

348

349 Neural Network (NN) Feature Selection:

350 The rudimentary neural network is built using PyTorch to feature select CpG sites, as neural
351 networks have been known to capture nonlinear relationships between data points. We were interested in
352 seeing what would be good predictors of aging that might have been missed by the other linear regression
353 models and lay the groundwork for future feature selection using NNs. As a proof-of-concept we used %-
354 RFE to reduce the number of features from 473,035 down to 100. The NN first uses all 100 original
355 features and trains the model once, its score being recorded as a benchmark. Following this, for each of
356 the 100 features, the NN is then trained twice; once where all methylation levels of that feature equals 1
357 and once where they all equal 0 to simulate the CpG being fully methylated and also absent. Both are
358 done to account for the cases where the original methylation value is close to 0 or 1. The mean of the two
359 resulting scores are compared to the benchmark with the difference being recorded for each CpG site.
360 The CpG sites are ranked in difference to establish an idea of feature importance with the postulation that

361 a larger difference between the presence and absence of the CpG will insinuate that the CpG has a greater
362 impact on age prediction. The top 50-75 are recorded as selected features.

363

364 Genetic Algorithm:

365 An algorithm based on the nature of Darwinism evolution where a population of ‘creatures’ are
366 assigned a desired amount of features from the original dataset at random. These creatures are evaluated
367 via predicting a validation set and assigned a score or ‘fitness’. The lowest scoring creatures are culled
368 next, simulating survival of the fittest. The remaining creatures are bred by creating a child creature that
369 has features from their shared ‘gene pool’ and having a new number of them selected randomly. There is
370 a chance for a certain number of these ‘genes’ to be mutated. Meaning some of the features will be
371 randomly swapped for a different one from the original dataset. This helps introduce variation. This
372 process is repeated for a specified number of generations or until a desired fitness is met.

373 The genetic algorithm is powerful as it allows the user many points of optimization, depending on
374 the creativity of the user. For instance, the number of generations, number of features and creatures are
375 all linked variables where a perfect balance can be found. When it comes to the breeding process it is
376 possible to implement a ‘polygamous’ aspect where a highly successful creature is allowed to breed
377 multiple times to ensure the most predictive features are passed on and tested further in other
378 combinations. Mutation rate, number of genes allowed to mutate as well as number of children produced
379 per breed (with possibility of scaling number of children produced with the fitness of the parent). It is
380 also common for genetic algorithms to be run in parallel, predicting subsets of a label, e.g. an algorithm
381 for young samples and one for old.

382

383 Novel methods combining multiple feature selection methods:

384 The introduction of %-RFE and to a lesser extent SFM allows us to synthesize novel feature
385 selection methods. %-RFE allows for the removal of ‘fluff’ down to a more manageable number of
386 features (usually a few thousand) and allows for more powerful methods to be used such as Boruta,

387 Neural Networks and RFECV. These methods require more iterations and computational power so being
388 able to distill down to the most important thousand features to choose from is ideal. The synthesized
389 methods consist of %-RFE first selecting features to an amount appropriate for the next method. SFM is
390 also used as a preliminary selection method in this way. The final synthesized methods consist of
391 modular code functions that allow us to alternate the order in which the selection methods are used as
392 well as let us combine them together and use the output of onemethod as the input of another.

393

394 Clock Models:

395 The epigenetic clocks are built using ElasticNetRegression models. ElasticNet is chosen as it is
396 the current standard for epigenetic clocks and outperforms Random Forests and SVMs with these data
397 and feature selection methods.

398 This model is a variant of classical linear regression. This aims to solve for the coefficients of a
399 linear equation that equals the 'best fit line'. The best fit line minimizes the sum of squares by having the
400 least distance between the data points and the line. The equation for ordinary linear regression is as
401 follows:

402
$$\text{argmin} = \sum (y_a - y_p)^2$$

403
$$\text{argmin} = \sum (y_a - (\beta_1 x_1 + \dots + \beta_n x_n) - b)^2$$

404 Where y_a is the actual value of the target label and prediction y_p calculated by the summation of
405 predictors ' x ' multiplied by a vector of coefficients β_n that is found from fitting the model b .
406 b is the y -intercept. argmin signifies a cost function where we seek to minimize the answer given input arguments.

407 Regularization is a process in which different variants of bias and penalties are introduced to
408 assist in finding the solution to this equation that allows for the best predictive accuracy. These penalties
409 are controlled by a lambda value (alpha in sklearn) that controls how heavy (large) this penalty is. The
410 L1 penalty is referred to as Lasso Regression, it adds a bias that is the absolute value of the coefficients.
411 The L2 penalty is referred to as Ridge regression, this adds a bias that is the squared value of the
412 coefficients. Unlike ridge regression, lasso regression can shrink the coefficients of unneeded parameters

413 (features) to 0 (due to the penalty term not being squared), essentially eliminating them, leaving only
414 useful features. Lasso can be quite aggressive however, taking only 1 feature out of several correlated
415 ones or selecting too few. This is where ElasticNet comes in. The generic form of the ElasticNet equation
416 is:

417
$$\text{argmin} = \sum (y_a - \beta x_n)^2 + \lambda_1 \sum |\beta| + \lambda_2 \sum \beta^2$$

418 Where L1 is the regularization penalty for the 'Lasso' part of the regression equation and L2 is the penalty
419 for the 'Ridge' portion (Zou, Hastie. 2005). ElasticNet combines both Lasso and Ridge regressions,
420 adding both terms to the equations. Each penalty gets an independent alpha / lambda that is tuned via
421 cross-validation or other methods. This method allows the best of both worlds depending on the feature.
422

423 **Acknowledgements:** D.A.S. was supported by the Glenn Foundation for Medical Research; A.E.K was
424 supported by a K99 award from the NIH (K99 AG070102); A.M. was supported by an F32 Ruth L.
425 Kirschstein National Research Service Award (NRSA) Individual Postdoctoral Fellowship from the NIH
426 (F32 AG069363);

427 D.V. received financial support from the NIDDK Mouse Metabolic Phenotyping Centers
428 (RRID:SCR_008997, MMPC, www.mmpc.org) under the MICROMouse Funding Program, grants
429 DK076169, and a NIH T32 grant T32AG023480.

430

431 **Conflict of Interests:** D.A.S. is a founder, equity owner, advisor to, director of, board member of,
432 consultant to, investor in and/or inventor on patents licensed to Revere Biosensors, UpRNA,
433 GlaxoSmithKline, Wellomics, DaVinci Logic, InsideTracker (Segterra), Caudalie, Animal Biosciences,
434 Longwood Fund, Catalio Capital Management, Frontier Acquisition Corporation, AFAR (American
435 Federation for Aging Research), Life Extension Advocacy Foundation (LEAF), Cohbar, Galilei, EMD
436 Millipore, Zymo Research, Immetas, Bayer Crop Science, EdenRoc Sciences (and affiliates Arc-Bio,
437 Dovetail Genomics, Claret Bioscience, MetroBiotech, Astrea, Liberty Biosecurity and Delavie), Life
438 Biosciences, Alterity, ATAI Life Sciences, Levels Health, Tally (aka Longevity Sciences) and Bold

439 Capital. D.A.S. is an inventor on a patent application filed by Mayo Clinic and Harvard Medical School
440 that has been licensed to Elysium Health. More information at <https://sinclair.hms.harvard.edu/david-sinclair-affiliations>.

442 **References:**

443
444 Bocklandt S, Lin W, Sehl ME, Sanchez FJ, Sinsheimer JS, Horvath S, et al. Epigenetic predictor of age.
445 PLoS One. 2011;6(6):e14821. doi:10.1371/journal.pone.0014821

446
447 Alghanim H, Antunes J, Silva D, Alho C, Balamurugan K, McCord B, 2017. Detection and evaluation of
448 DNA methylation markers found at SCGN and KLF14 loci to estimate human age. Forensic Science
449 International: Genetics, 31, pp.81-88.

450
451 Chen D, Chao D, Rocha L, Kolar M, Nguyen Huu V, Krawczyk M et al., 2020. The lipid elongation
452 enzyme ELOVL2 is a molecular regulator of aging in the retina. Aging Cell, 19(2).

453
454 Darst B., Malecki K, Engelmann C., 2018. Using recursive feature elimination in random forest to account
455 for correlated variables in high dimensional data. BMC Genetics, 19(S1).

456
457 Pedregosa F, Varoquaux G, Gramfort A, Michel V, Thirion B, Grisel O, et al., Scikit-learn: Machine
458 Learning in Python, JMLR 12, pp. 2825-2830, 2011.

459
460 Fleckhaus J, Schneider P., 2020. Novel multiplex strategy for DNA methylation-based age prediction
461 from small amounts of DNA via Pyrosequencing. Forensic Science International: Genetics, 44, p.102189.

462

463 Graf GH, Crowe CL, Kothari M, Kwon D, Manly JJ, Turney IC, et al. (2021) 'Testing Black-White
464 disparities in biological aging in older adults in the United States: analysis of DNA-methylation and
465 blood-chemistry methods', *American journal of epidemiology*. doi: 10.1093/aje/kwab281

466

467 Griffin PT, Kane AE, Trapp A, Li J, McNamara MS, Meer MV, et al. (2021) 'Ultra-cheap and scalable
468 epigenetic age predictions with TIME-Seq', *bioRxiv*. doi: 10.1101/2021.10.25.465725.

469 Guyon I, Elisseeff A, An Introduction to Variable and Feature Selection; *Journal of Machine Learning*
470 *Research* 3 (2003) 1157-1182

471

472 Hannum G, Guinney J, Zhao L, Zhang L, Hughes G, Sadda S, et al. 2013. Genome-wide Methylation
473 Profiles Reveal Quantitative Views of Human Aging Rates. *Molecular Cell*, 49(2), pp.359-367.

474

475 Hosoda Y, Yoshikawa M, Miyake M, Tabara Y, Shimada N, Zhao W, et al. 2018. CCDC102B confers
476 risk of low vision and blindness in high myopia. *Nature Communications*, 9(1).

477

478 Horvath S., 2013. DNA methylation age of human tissues and cell types. *BMC*
479

480 Horvath S, Garagnani P, Bacalini M, Pirazzini C, Salvioli S, Gentilini D, et al. 2015. Accelerated
481 epigenetic aging in Down syndrome. *Aging Cell*, 14(3), pp.491-495.

482

483 Ito H, Udono T, Hirata S, Inoue-Murayama M, 2018. Estimation of chimpanzee age based on DNA
484 methylation. *Scientific Reports*, 8(1).

485

486 Iwaya, C., Kitajima, H., Yamamoto, K., Maeda, Y., Sonoda, N., Shibata, H. and Inoguchi, T., 2018.
487 DNA methylation of the Klf14 gene region in whole blood cells provides prediction for the chronic

488 inflammation in the adipose tissue. *Biochemical and Biophysical Research Communications*, 497(3),
489 pp.908-915.

490

491 Kursa MB, Rudnicki WR 2010. "Feature Selection with the Boruta Package." *Journal of Statistical*
492 *Software*, 36(11), 1–13

493

494 Levine ME, Lu AT, Quach A, Chen BH, Assimes TL, Bandinelli S et al. (2018). An epigenetic
495 biomarker of aging for lifespan and healthspan. *Aging*, 10(4), 573–591.

496

497 Lu A, Quach A, Wilson J, Reiner A, Aviv A, Raj K, et al. 2019. DNA methylation GrimAge strongly
498 predicts lifespan and healthspan. *Aging*, 11(2), pp.303-327.

499

500 Moore L, Le T, Fan G, (2012). DNA Methylation and Its Basic Function. *Neuropsychopharmacology*,
501 38(1), 23-38. doi: 10.1038/npp.2012.112

502

503 Mathgene.usc.es. 2021. Age prediction with DNA methylation: blood, 7 CpGs, EpiTYPER. [online]
504 Available from: http://mathgene.usc.es/cgi-bin/snps/age_tools/processmethylation-first.cgi.

505

506 Martens CR, Lubieniecki KL, McNamara MN, Bohr AD, McQueen MB, Seals DR, (2020) 'Epigenetic
507 patterns with aging and exercise are associated with indicators of healthspan in humans' National Center
508 for Biotechnology Information. U.S. National Library of Medicine; [online] Available from:
509 <https://www.ncbi.nlm.nih.gov/geo/query/acc.cgi?acc=GSE85311>

510

511

512 McEwen L, O'Donnell K, McGill M, Edgar R, Jones M, MacIsaac J, et al. (2019). The PedBE clock
513 accurately estimates DNA methylation age in pediatric buccal cells. *Proceedings Of The National
514 Academy Of Sciences*, 117(38), 23329-23335. doi: 10.1073/pnas.1820843116

515

516 Meer MV, Podolskiy DI, Rashkovskiy A, Gladyshev VN (2018). A whole lifespan mouse multi-tissue
517 DNA methylation clock. *ELife*, 7, 1–16.

518

519 Meng H, Murrelle E, Li G, 2008. Identification of a small optimal subset of CpG sites as bio-markers
520 from high-throughput DNA methylation profiles. *BMC Bioinformatics*, 9(1), p.457.

521

522 Park JL, Kim JH, Seo E, Bae DH, Kim SY, Lee HC, et al. Identification and evaluation of age-correlated
523 DNA methylation markers for forensic use. *Forensic Sci Int Genet*. 2016;23:64–70. doi:
524 10.1016/j.fsigen.2016.03.005.

525

526 Petkovich DA, Podolskiy DI, Lobanov AV, Lee SG, Miller RA, Gladyshev VN (2017). Using DNA
527 Methylation Profiling to Evaluate Biological Age and Longevity Interventions. *Cell Metabolism*, 25(4),
528 954-960.e6

529

530 Renner M, Wolf T, Meyer H, Hartmann W, Penzel R, Ulrich A, et al. 2013. Integrative DNA methylation
531 and gene expression analysis in high-grade soft tissue sarcomas. *Genome Biology*, 14(12), p.r137.

532

533 Schultz M, Kane A, Mitchell S, MacArthur M, Warner E, Vogel D, et al. 2020. Age and life expectancy
534 clocks based on machine learning analysis of mouse frailty. *Nature Communications*, 11(1).

535

536 Spólnicka M, Pośpiech E, Pepłońska B, Zbieć-Piekarska R, Makowska Ż, Pięta A, et al. 2017. DNA
537 methylation in ELOVL2 and C1orf132 correctly predicted chronological age of individuals from three
538 disease groups. *International Journal of Legal Medicine*, 132(1), pp.1-11.

539

540 Stubbs TM, Bonder MJ, Stark AK, Krueger F, von Meyenn F, Stegle O, et al. (2017). Multi-tissue DNA
541 methylation age predictor in mouse. *Genome Biology*, 18(1), 1–14.

542

543 Tharakan R, Ubaida-Mohien C, Moore A, Hernandez D, Tanaka T, Ferrucci L, 2020. Blood DNA
544 Methylation and Aging: A Cross-Sectional Analysis and Longitudinal Validation in the InCHIANTI
545 Study. *The Journals of Gerontology: Series A*, 75(11), pp.2051-2055.

546

547 Thompson M, Chwialkowska K, Rubbi L, Lusis A, Davis R, Srivastava A, et al. (2018). A multi-tissue
548 full lifespan epigenetic clock for mice. *Aging*, 10(10), 2832-2854. doi: 10.18632/aging.101590

549 Trapp A, Kerepesi C, Gladyshev VN (2021) 'Profiling epigenetic age in single cells', *Nature Aging*, pp.
550 1–13. doi: 10.1038/s43587-021-00134-3.

551

552 Voisin S, Harvey N, Haupt L, Griffiths L, Ashton K, Coffey V, et al. 2020. An epigenetic clock for
553 human skeletal muscle. *Journal of Cachexia, Sarcopenia and Muscle*, 11(4), pp.887-898.

554

555 Wang Y, Deng H, Xin S, Zhang K, Shi R, Bao X, 2018. Prognostic and Predictive Value of Three DNA
556 Methylation Signatures in Lung Adenocarcinoma. *SSRN Electronic Journal*,

557

558 Weidner CI, Lin W, Koch CM., Eisele L, Beier F, Ziegler P, et al. (2014) 'Aging of blood can be tracked
559 by DNA methylation changes at just three CpG sites', *Genome biology*, 15(2), p. R24. doi: 10.1186/gb-
560 2014-15-2-r24.

561

562 Xia Y, Huang N, Chen Z, Li F, Fan G, Ma D, et al. 2018. CCDC102B functions in centrosome linker
563 assembly and centrosome cohesion. *Journal of Cell Science*, 131(23), p.jcs222901.

564

565 Yin J, Chen W, Chao E, Soriano S, Wang L, Wang W, et al. 2018. *Otud7a Knockout Mice Recapitulate*
566 *Many Neurological Features of 15q13.3 Microdeletion Syndrome*. *The American Journal of Human*
567 *Genetics*, 102(2), pp.296-308.

568

569 Zbieć-Piekarska R, Spólnicka M, Kupiec T, Makowska Ż, Spas A, Parys-Proszek A, et al. Examination
570 of DNA methylation status of the ELOVL2 marker may be useful for human age prediction in forensic
571 science. *Forensic Science International: Genetics*, 14, pp.161-167.

572

573 Zbieć-Piekarska R, Spólnicka M, Kupiec T, Parys-Proszek A, Makowska Ż, Pałeczka A, et al. 2015.
574 Development of a forensically useful age prediction method based on DNA methylation analysis. *Forensic*
575 *Science International: Genetics*, 17, pp.173-179.

576

577 Zou H, Hastie T, 2005. Regularization and variable selection via the elastic net. *Journal of the Royal*
578 *Statistical Society: Series B (Statistical Methodology)*, 67(2), pp.301-320.

579

580

581

582

583

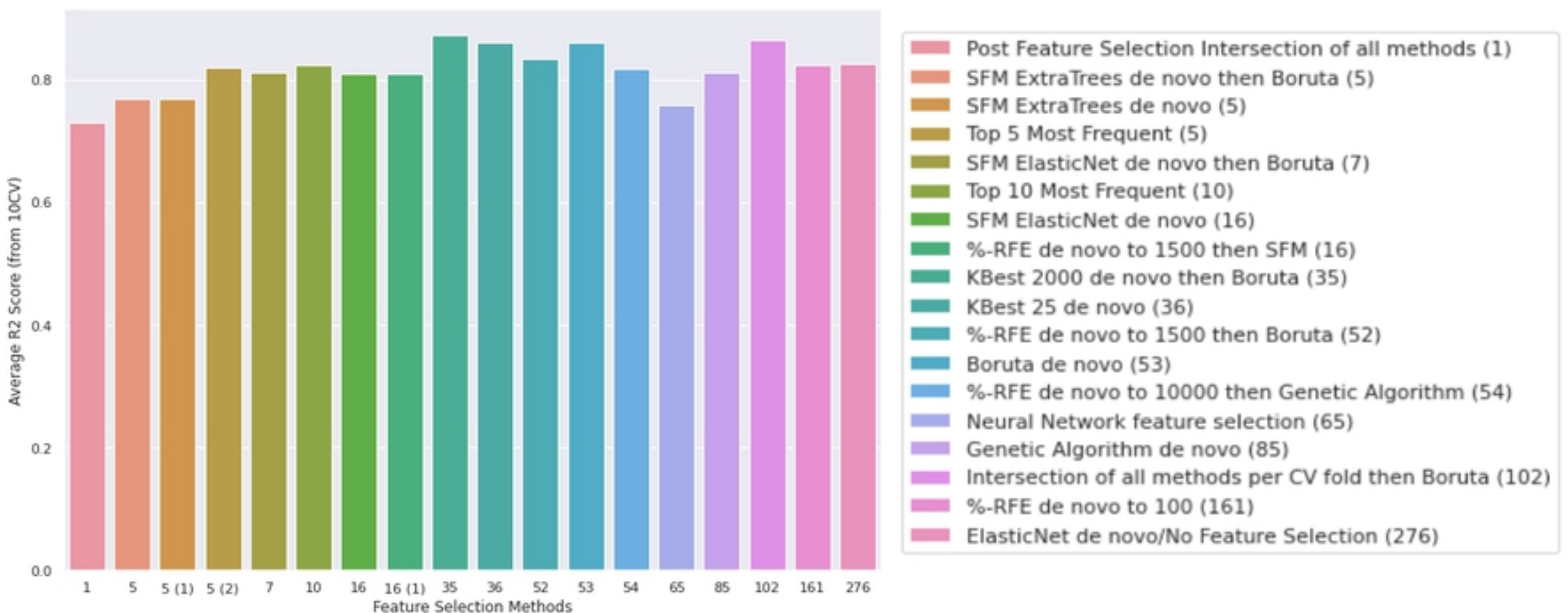
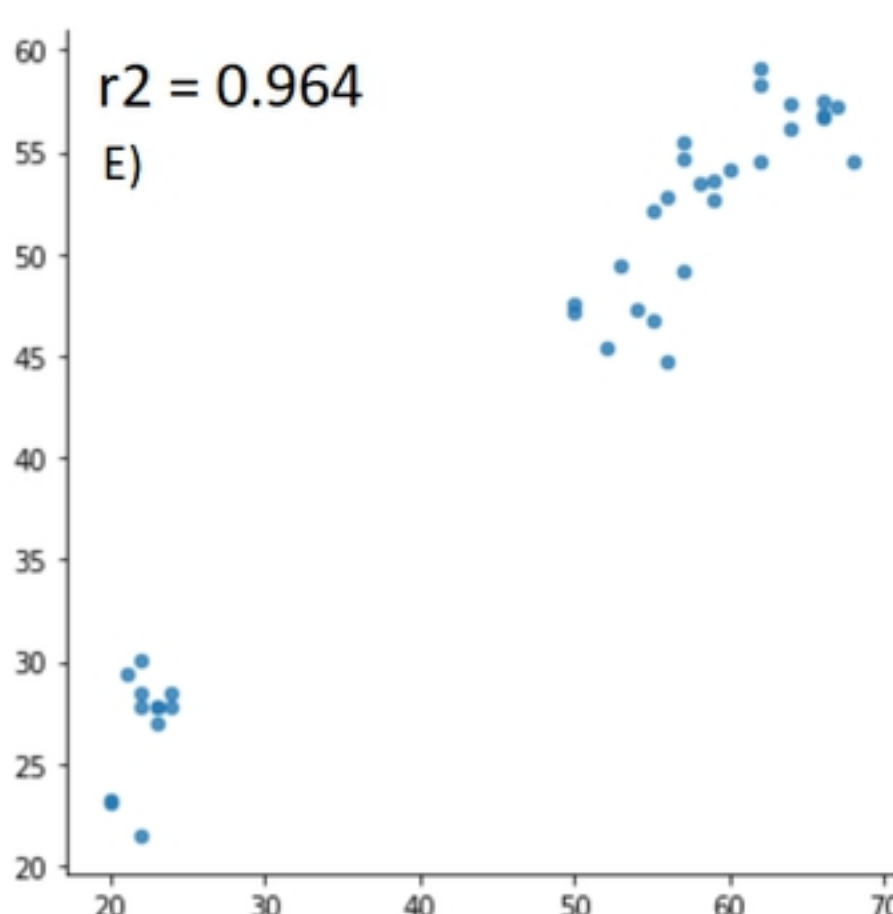
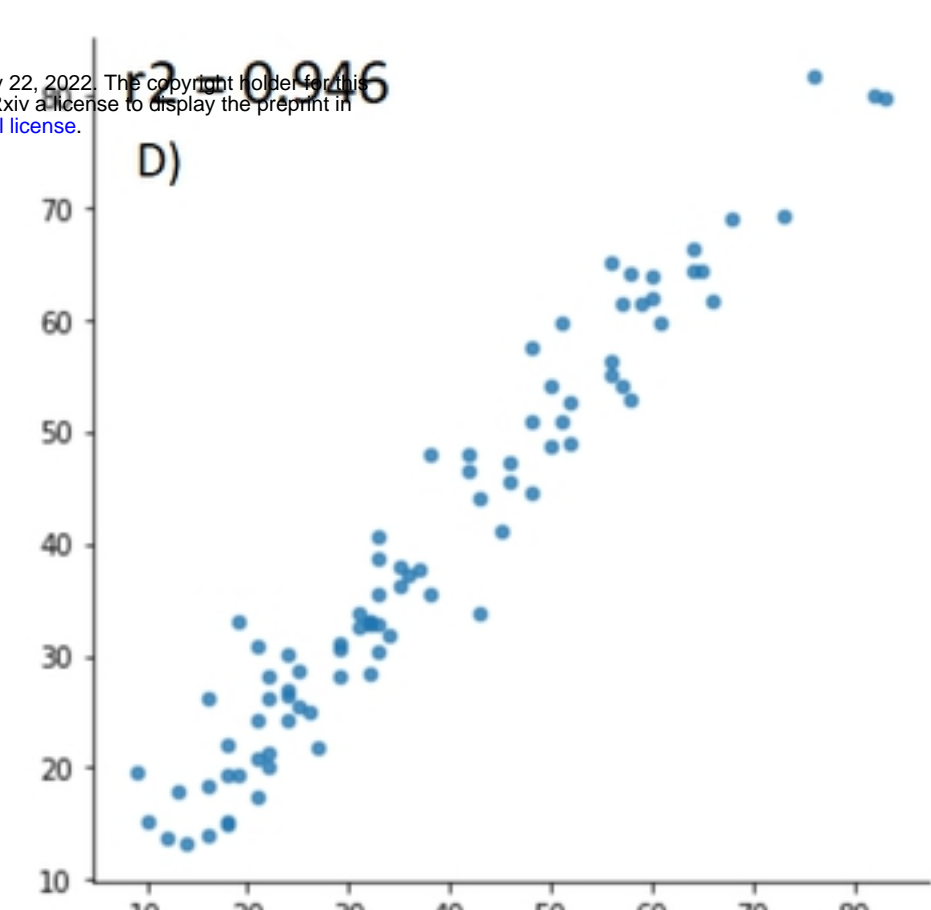
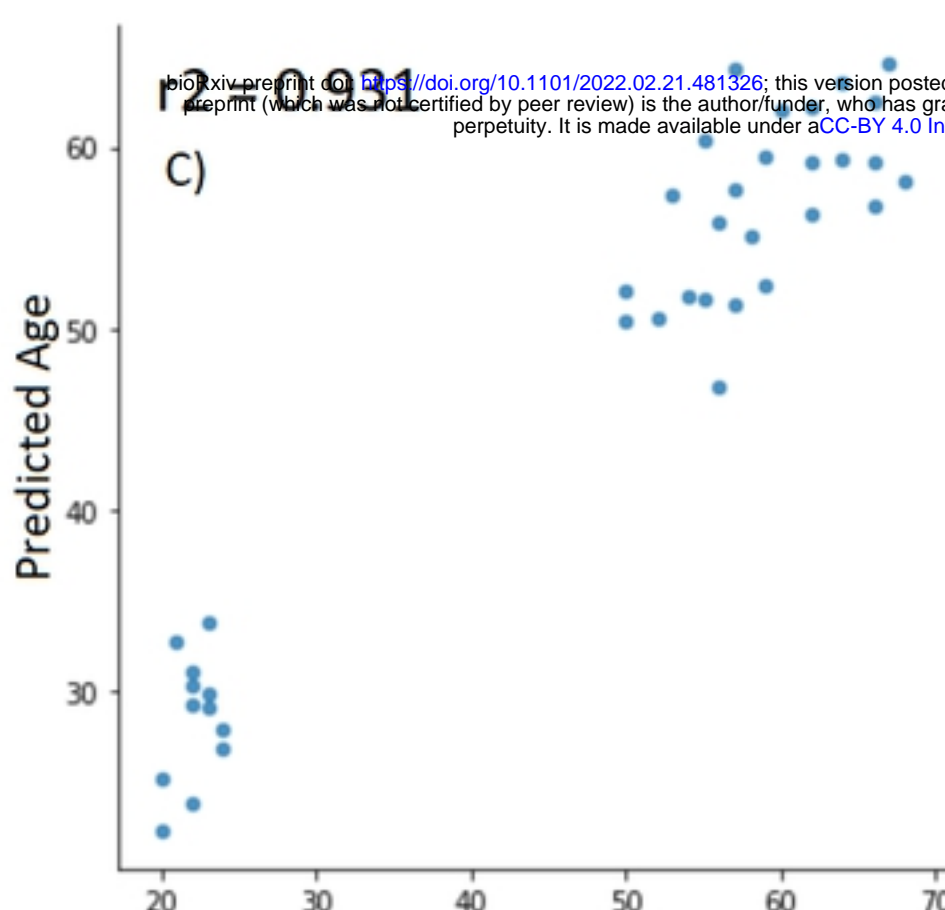
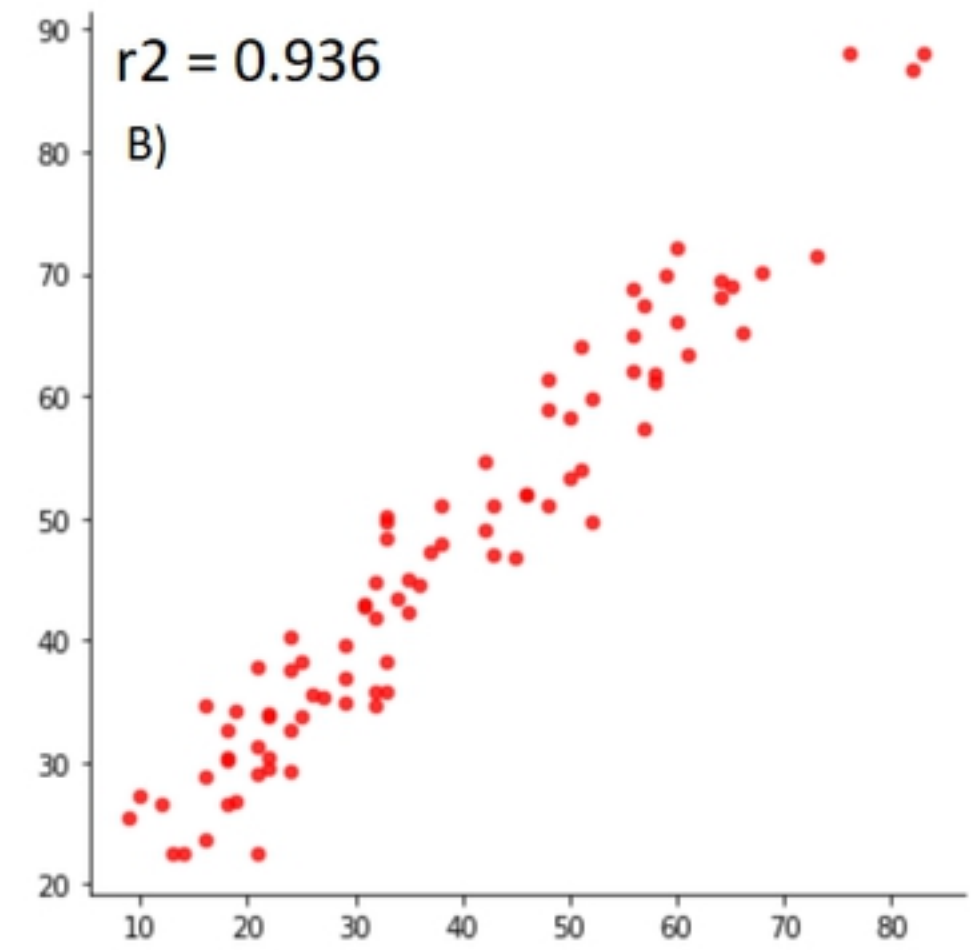
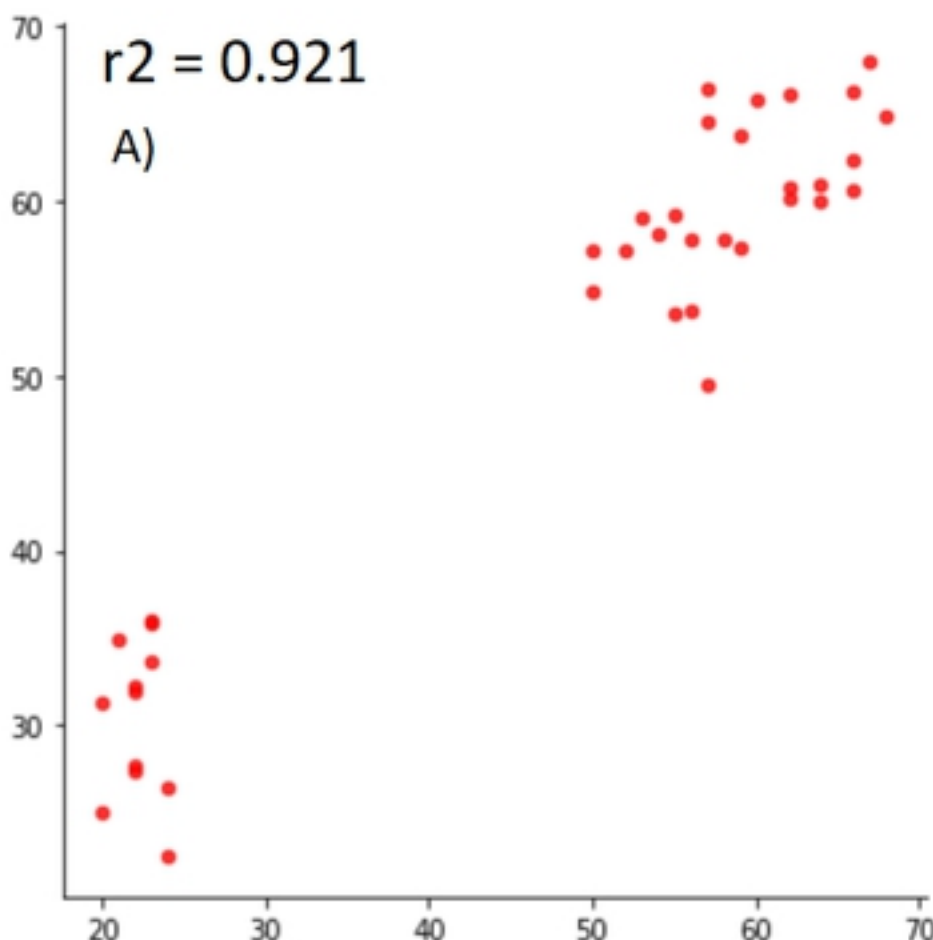
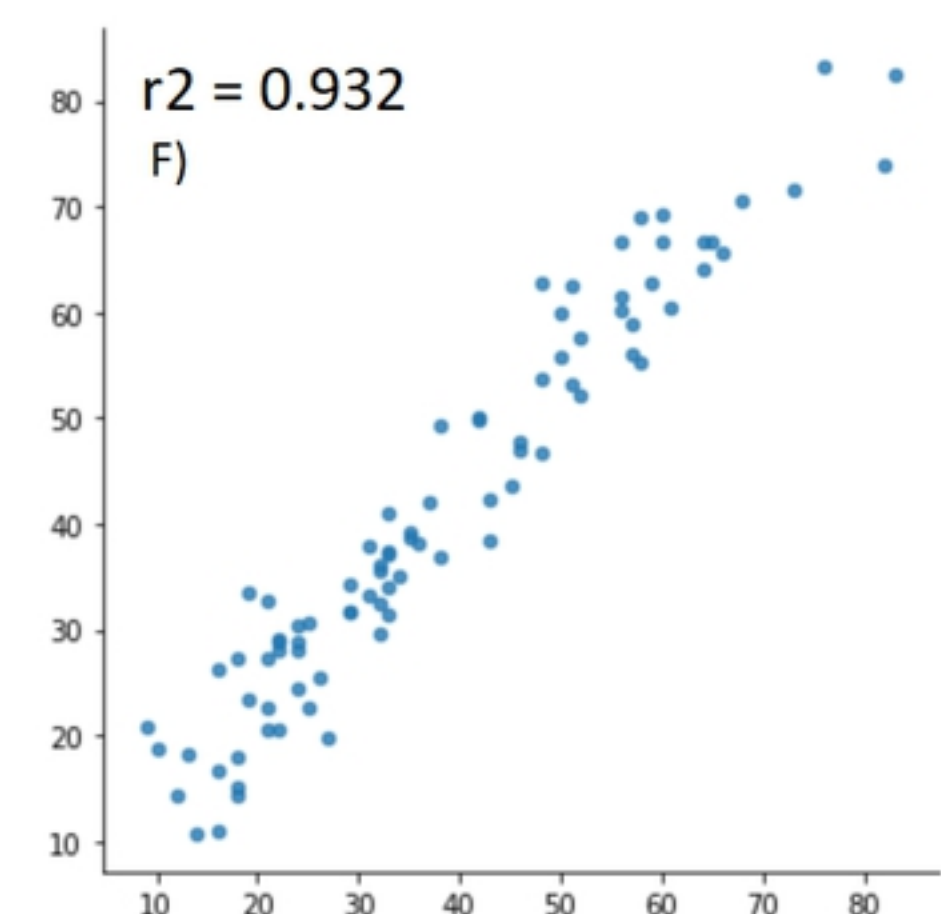


Figure 1



GSE85311



GSE52588

START

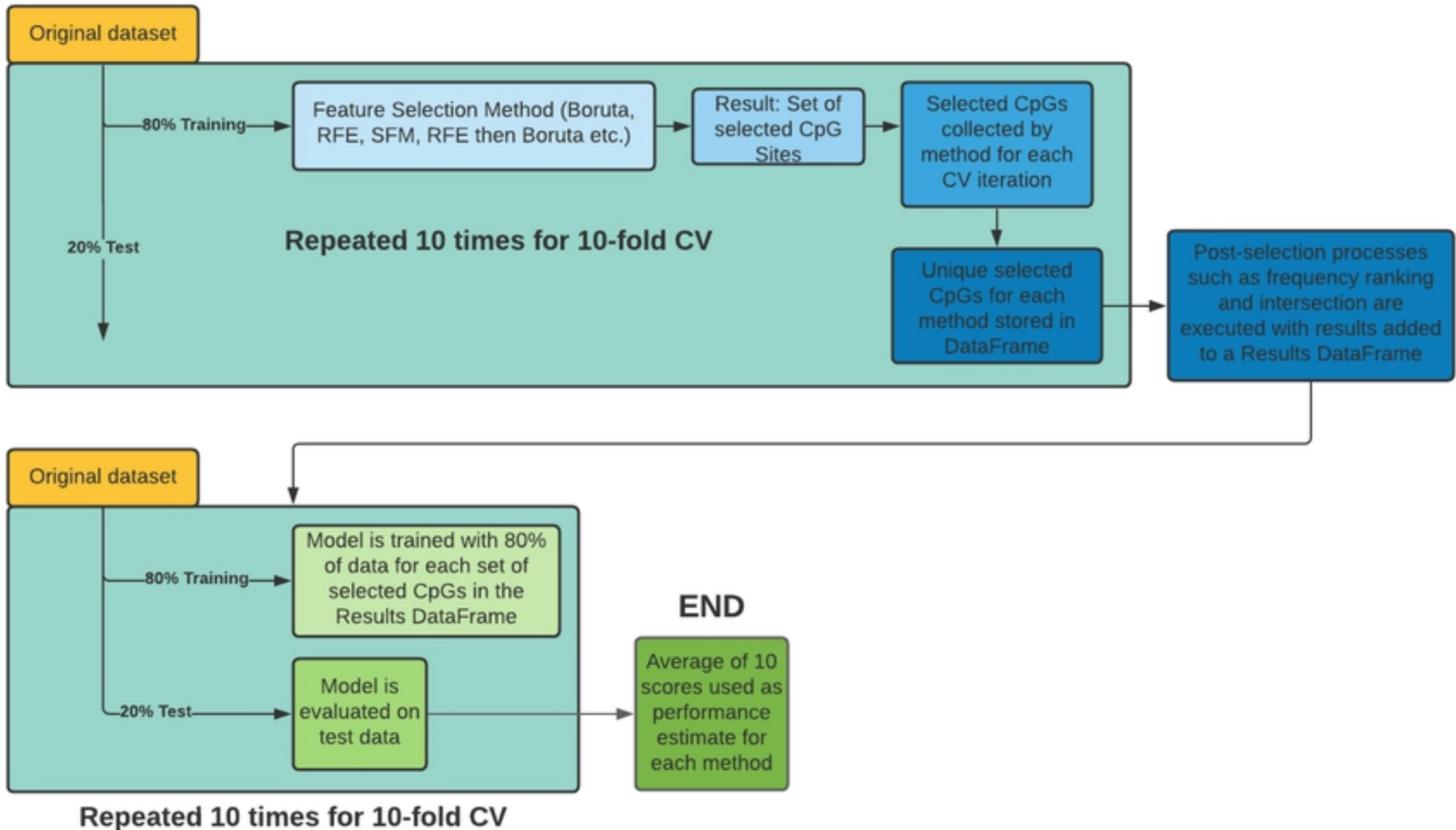


Figure 3